

# Preparation and characterization of polyacrylonitrile / antimony doped tin oxide composite nanofibers by electrospinning method

WEI PAN\*, XIAOWEI HE, YAN CHEN

*School of Materials and Chemical Engineering, Zhongyuan University of Technology, Zhengzhou 450007, P. R. China*

Polyacrylonitrile (PAN)/Antimony Doped Tin Oxide (ATO) composite nanofibers were prepared by electrospinning composite solutions of ATO and PAN in N,N-dimethylformamide (DMF). The surface morphology, thermal properties and crystal structure of PAN/ATO nanofibers are characterized using Fourier transform infrared spectroscopy (FTIR), wide-angle x-ray diffraction (WAXD), scanning electron microscopy (SEM), Thermo gravimetric analyses (TGA) and differential scanning calorimetry (DSC). The results indicate that the introduction of ATO nanoparticles into the polymer matrix has a significant effect on the crystallinity of PAN and a strong interaction between PAN and ATO nanoparticles.

(Received January 31, 2010; accepted March 12, 2010)

*Keywords:* Electrospinning, PAN, ATO, Nanofibers

## 1. Introduction

Composite nanofibers, consisting of nanoscale inorganic fillers and polymer matrix, combine the advantages of both the polymer materials, such as light weight, flexibility, and good moldability, and the inorganic materials, such as high strength, heat stability, and chemical resistance [1, 2]. As a result, these composite nanofibers can have enhanced mechanical, electrical, optical, thermal and magnetic properties without losing transparency, and they can be excellent candidates for many multifunctional applications that include membranes, biomedical devices, and energy conversion and storage systems [2–4].

Many methods have been used to prepare composite nanofibres [5–9]. Among these, electrospinning is an effective and simple method for preparing various polymer/inorganic composite nanofibres. The electrospinning technique has been developed since 1934 for the synthesis of nanofibres. It is a process which uses a strong electrostatic force by a high static voltage applied to a polymer solution placed into a container that has a millimeter diameter nozzle. Under applied electrical force, the polymer solution is ejected from the nozzle. After the solvents are evaporated during the course of jet spraying, the nanofibres are collected on a grounded collector. As a result, nanoscale thin fibres are obtained [10–12].

Polyacrylonitrile (PAN) is an important engineering polymer material that has been widely used to produce a variety of synthetic fibers. However, strong static electricity makes PAN to absorb dust and microbes easily. The electrical conductivity of insulating materials can be increased by the addition of electrically conductive fillers. A particularly interesting conductive filler is antimony doped tin oxide (ATO) as it combines a good electrical conductivity with optical transparency. The

combination of optical transparency and high electrical conductivity is important for applications like in solar cells, light emitting diodes, and permanent anti-static coatings. ATO has been used to increase the electrical conductivity of polyvinyl acetate-acrylate copolymer coatings [13], poly (methyl methacrylate) [14], and polyacrylonitrile films [15].

In the present study, PAN solutions in N, N-dimethylformamide containing ATO nanoparticles were first prepared, and then electrospun into PAN/ATO composite nanofibers. The surface morphology, thermal stability, and crystal (phase) structure of the PAN/ATO nanocomposite fibers are characterized by various techniques, including attenuated total reflection Fourier transform infrared (FT-IR) spectroscopy, scanning electron microscopy (SEM), and X-ray diffraction (XRD).

## 2. Experimental

The PAN ( $M_w=5.5 \times 10^4$ ) employed in this study was purchased from Shanghai petroleum Chemical Co., Ltd (Shanghai, China). The untreated nano-ATO particles with specific surface area  $80 \text{ m}^2/\text{g}$  were purchased from Shanghai Huzheng Technology Co., Ltd. (Shanghai, China). The silane coupling agent (KH570, commercial grades) was supplied by Shanghai Yaohua Chemical Plant (Shanghai, China), which was used to treat the nano-ATO particles. Other agents and process assistants (commercial grades) were obtained from the market.

Silane coupling agent (0.2 g) was mixed with 5.0 g distilled water and 95.0 g absolute ethanol, and then 10.0 g ATO powder was added into the solvent mixture. The suspension was dispersed in an ultrasonicator for 1 h. The suspension was refluxed at 120 for 24 h. After surface treatment, the Nano-ATO particles were rinsed with

ethanol three times in order to remove any unreacted silane coupling agent.

PAN was dissolved in DMF at 60 °C and the concentration was fixed at 7 wt%. A controlled amount of ATO nanoparticles were dispersed into PAN solution in DMF. Mechanical stirring was applied for at least 10 h at 60 °C in order to obtain homogeneous ATO dispersed PAN solutions. Composite solutions were fed through a capillary tip (diameter = 0.5mm) using a syringe (30 ml). The anode of the high voltage power supply was clamped to a syringe needle tip and the cathode was connected to a metal collector. During electrospinning, the applied voltage was 14 kV, the distance between the tip and collector was 17 cm, and the flow rate of the spinning solution was 1 ml/h.

The diameter and morphology of the electrospun PAN/ATO composite fibers were determined by a JSM-5610 scanning electron microscope (SEM, Japan). Wide angle X-ray diffraction was carried out using a BRUKER-AXC08 X-ray diffractometer and filtered CuK $\alpha$  radiation. The diffraction patterns of the composite fibers of the ATO and PAN were obtained by scanning the samples in an interval of  $2\theta = 10$ -60 degrees. Fourier transform infrared (FTIR) spectra were collected from a FTIR spectrometer (Nicolet 560) in the wavenumber range of 4000–700  $\text{cm}^{-1}$ . Thermal properties of electrospun fibers were evaluated using differential scanning calorimetry (DSC) from 40 to 380 at a heating rate of 20  $\text{min}^{-1}$  in nitrogen environment. Thermo gravimetric analyses of pure PAN and PAN/ATO composite fibers were performed with a TA Instruments Du Pont 1090 at 10°C/min under air atmosphere.

### 3. Results and discussion

In the process of electrospinning, the addition of nanoparticles has significant influence on the fiber morphological characteristics such as fiber diameter, surface roughness, and fiber orientation. Fig. 1 shows SEM images a of pure PAN and PAN/ATO composite nanofibers electrospun from 7 wt% PAN solutions with different ATO concentrations at a fixed voltage of 14 kV. It is seen that all fibers are relatively uniform and randomly oriented, forming an interwoven network on the substrate. Defects, such as beads or fibers with 'beads on a string' morphology, can seldom be seen when the ATO concentration is lower than 15 wt%. A small number of bead-like irregularities appear in the nanofibers spun from solutions with 15 wt% ATO concentration. The average fiber diameter of pure PAN is about 270 nm. When the ATO content increases from 2 to 5, 10 and 15 wt%, the average fiber diameter becomes gradually thinner from 140 to 125, 110 and 100 nm, respectively. Conversely, in the case of 20 wt% ATO, the average fiber diameter increases to 180 nm, and the surface roughness also increases.

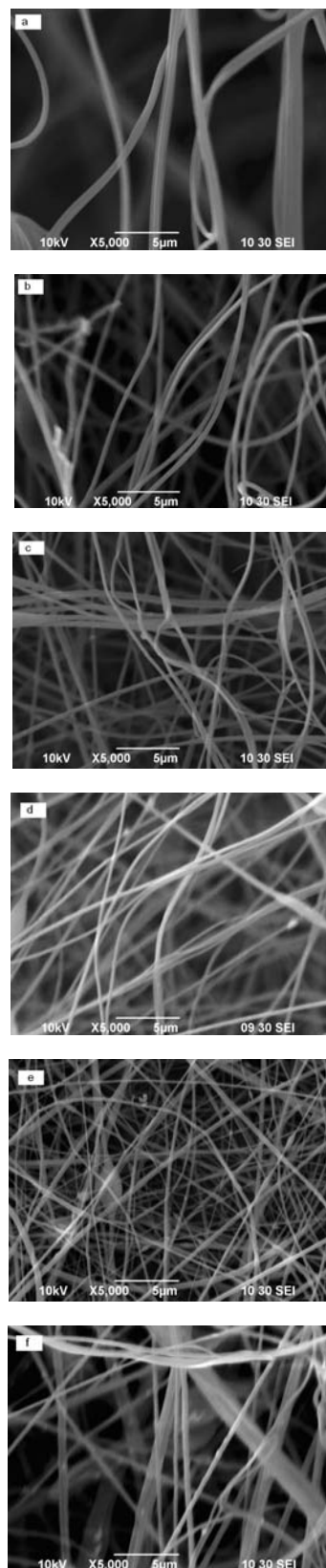


Fig. 1. SEM images of PAN/ATO composite nanofibers with different ATO contents. (a) 0 wt% (pure PAN), (b) 2 wt%, (c) 5 wt%, (d) 10 wt%, (e) 15 wt% and (f) 20 wt%.

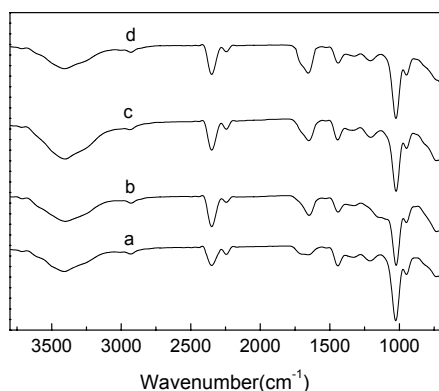


Fig. 2 FTIR spectra of PAN/ATO composite nanofibers with different ATO contents. (a) 0 wt% (pure PAN), (b) 5 wt %, (c) 10 wt%, and (d) 20 wt%.

FT-IR spectra of the pure PAN and PAN/ATO nanocomposites with different nanoparticle loadings were recorded in the range 4000-700  $\text{cm}^{-1}$ . All of the FT-IR spectra, Fig. 2, exhibit the PAN characteristic peaks such as the stretching vibration of nitrile groups (-CN-) at 2244  $\text{cm}^{-1}$  and the stretching vibration and bending vibration of methylene (-CH<sub>2</sub>-) peaks at 2930 and 1453  $\text{cm}^{-1}$ , respectively [16, 17]. The peak at 1670  $\text{cm}^{-1}$  is due to the oxidation of the as-received PAN in air, which results in the formation of carboxyl (C=O) groups. The peaks at 1251 and 1360  $\text{cm}^{-1}$  are assigned to the aliphatic CH group vibrations of different modes in CH and CH<sub>2</sub>, respectively. The positions of these peaks in PAN/ATO composite nanofibers shift to slightly lower values due to the interaction between PAN molecules and ATO. The peak intensity of the C=O stretching observed at about 1670  $\text{cm}^{-1}$  increases greatly with increase in ATO concentration. These phenomena indicate that nano-ATO and possibly the PAN molecules interact with the solvent DMF [18].

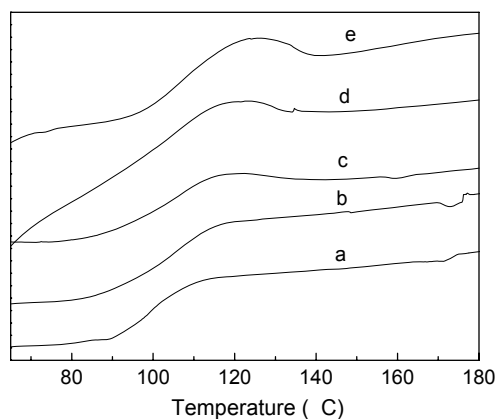


Fig. 3. DSC curves of PAN/ATO composite nanofibers in the range of 65-180 °C, the ATO content are (a) 0 wt% (pure PAN), (b) 5 wt%, (c) 10 wt%, (d) 15 wt% and (e) 20 wt%.

DSC thermograms of pure PAN and PAN/ATO nanofibers are in the range of 65-180°C presented in fig. 3. It shows that  $T_g$  of the nanocomposites shift to higher temperature with the increasing of nano-ATO content. Such an effect on  $T_g$  has been reported to obey motion restrictions of the polymer chains in the nanoparticle matrix interface [19]. When the polymer chains present strong interfacial affinity with the filler, a region of strongly bound polymer chains is formed. This region has been speculated to be within a few nanometers and called the “bound polymer layer” [20] at higher lengths, it has been called the “interaction zone”. In this zone or region, the polymer chains exhibit a different behavior than that in bulk; the strong packing hinders chain segmental mobility, which occurs under standard conditions at  $T_g$ . Thus, more energy is required to allow the first thermal transition, shifting  $T_g$  to a higher temperature.

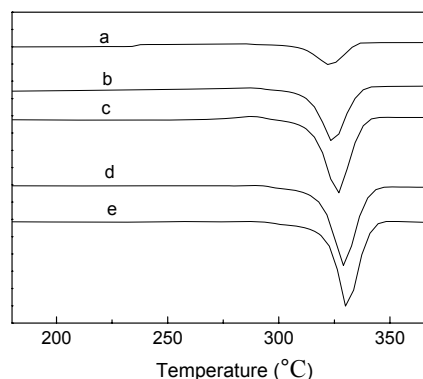


Fig. 4. DSC curves of PAN/ATO composite nanofibers in the range of 180-380 °C, the ATO content were (a) 0 wt% (pure PAN), (b) 5 wt%, (c) 10 wt%, (d) 15 wt% and (e) 20 wt%.

DSC thermograms of pure PAN and PAN/ATO nanofibers are in the range of 180-380°C presented in fig.4. All nanofiber samples exhibit a relatively large exothermic peak. With increase in ATO content, the exothermic peak became shaper and shift to higher temperatures. This peak can result from a combination of three principal reactions, namely dehydrogenation, instantaneous cyclization and crosslinking reactions, which are exothermic in nature [21]. Among these three reactions, the predominant process is the instantaneous cyclization of the nitrile groups into an extended conjugated ring system. The fast reaction of PAN nanofibers in nitrogen may be due to the facile formation of free radicals on the nitrile groups and subsequent recombinations between the radicals intermolecularly or intramolecularly [22]. Increases in peak temperature for PAN/ATO composite nanofibers may be caused by the inhibiting effect of ATO nanoparticles, which hinder the recombinations between the radicals

The crystalline properties of electrospun fibers are

important when the materials are designed and fabricated for commercial applications. In order to investigate the crystalline structure of the PAN and ATO nanoparticles in the electrospun PAN nanocomposite fibers, XRD measurements were performed. Fig.5 presents XRD characterizations of nano-ATO. The X-ray patterns of the nano-ATO displayed the presence of five peaks at  $2\theta = 26.5^\circ$ ,  $33.7^\circ$ ,  $37.7^\circ$ ,  $51.7^\circ$  and  $54.7^\circ$  corresponding to the reflection of (110), (101), (200), (220) and (211) [23].

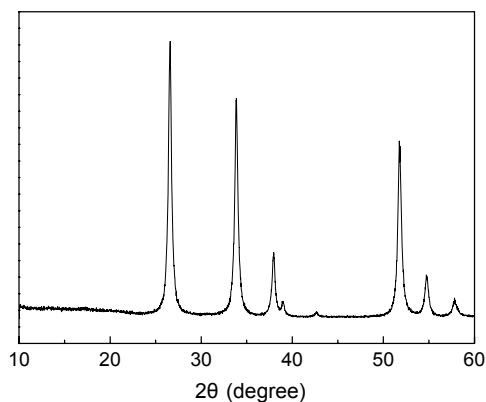


Fig. 5. XRD patterns of nano-ATO.

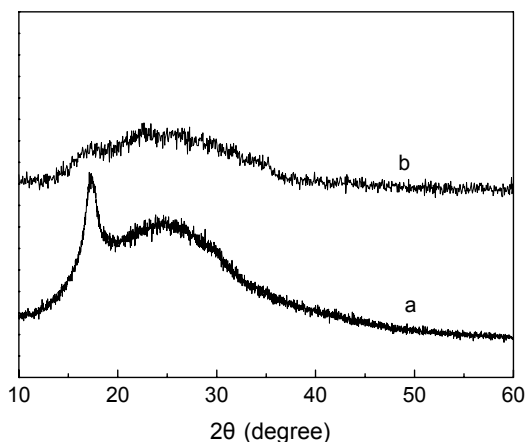


Fig. 6. XRD patterns of the (a) as-received pure PAN powder and (b) electrospun pure PAN fiber.

Fig. 6 shows the XRD patterns of the as-received pure PAN powder and electrospun pure PAN fiber. The XRD pattern of the as-received pure PAN powder shows a diffraction peak at  $2\theta = 17^\circ$ . We found the crystallinity of PAN nanofibers was lower than PAN powder. This phenomenon confirmed the electrospinning retarded the crystallization process of polymer, which did not lead to the development of the crystalline microstructure of electrospun fiber. The reason for the retardation could be explained as following. During electrospinning, the stretched molecular chains of the fiber solidified rapidly at

high elongate rates, which significantly hindered the formation of crystals.

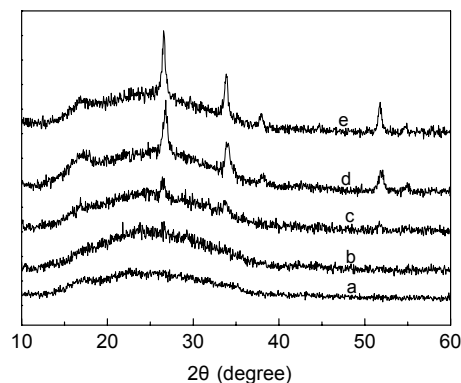


Fig. 7. XRD patterns of PAN/ATO composite nanofibers with different ATO contents. (a) 0 wt% (pure PAN fiber), (b) 5 wt%, (c) 10 wt%, (d) 15 wt% and (e) 20 wt%.

The XRD characterizations of PAN/ATO composite nanofibers with 4 different ATO content were conducted (see Fig. 7). The intensity of the peaks assigned to the nano-ATO and the peak at  $2\theta = 17^\circ$  in the composite nanofibers increased with the increase of the content of nano-ATO. These observations indicate a large influence of ATO nanoparticles on the crystallinity of PAN in the composite fibers and a strong interaction between the nanoparticles and the polymer matrix.

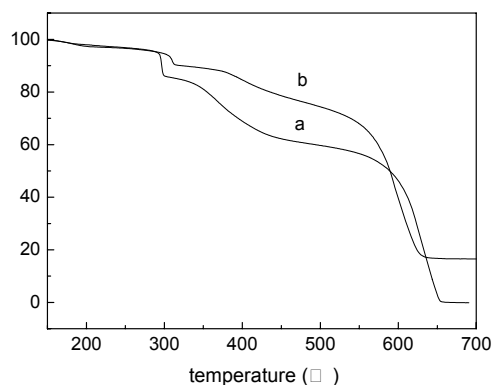


Fig. 8. TGA curves of (a) pure PAN nanofiber and (b) PAN/ATO (10 wt %) composite nanofiber.

The TGA curves for the pure PAN nanofiber and PAN/ATO composite nanofiber with 8wt% nano-ATO content in atmosphere are shown in Fig. 8. There are two obvious weight loss peaks at 290-320 °C and 600-640 °C in the TGA curves. The first weight loss is caused by decarboxylation of the methylacrylate in Co-PAN and the second weight loss is due to thermo-oxidative degradation of PAN macromolecular chains. It is observed in Fig. 8 that the first thermal decomposition temperature of PAN/ATO composite fiber with 10wt% ATO content is around 324 °C, whereas that of neat PAN fiber is only 308 °C. This clearly demonstrates that the PAN/ATO system is

thermally more stable than the corresponding neat PAN system. This means that the incorporation of nano-ATO into PAN offers a stabilizing effect against the decomposition.

#### 4. Conclusions

Various PAN/ATO composite fibers were prepared by electrospinning composite solutions containing nano-ATO and polyacrylonitrile (PAN) in N, N dimethylformamide (DMF). FTIR, DSC and TGA curves reveal that there are interactions among PAN chain and ATO. These interactions have profound effects on the thermal properties of nanofibers. It is found that the amount of ATO nanoparticles could affect the thermal stabilities and the glass transition temperature of PAN. As the mass ratio of Ag nanoparticles increased, the glass transition temperature increased. The PAN/ATO composite nanofiber is thermally more stable than the corresponding neat PAN fiber.

#### References

- [1] Y. Dzenis, *Science* **34**, 1917 (2004).
- [2] K. M. Sawicka, P. Gouma, *J. Nanopart. Res.* **8**, 769 (2006).
- [3] Y. Z. Wang, Y. X. Li, S. T. Yang, G. L. Zhang, D. M. An, C. Wang, Q. B. Yang, X. S. Chen, *Nanotechnology* **17**, 3304 (2006).
- [4] D. Li, Y. N. Xia, *Adv. Mater.* **16**, 1151 (2004).
- [5] J. F. Wang, M. S. Gudixsen, X. F. Duan, Y. Cui, C. M. Lieber, *Science* **293**, 1455 (2001).
- [6] C. Drew, X. Liu, D. Ziegler, X. Wang, F. F. Bruno, J. Whitten, L. A. Samuelson, *Nano Lett.* **3**, 143 (2003).
- [7] T. Cui, F. Cui, J. Zhang, J. Wang, J. Huang, C. Lu, Z. Chen, B. Yang, *J. Am. Chem. Soc.* **128**, 6298 (2006).
- [8] J. Zhang, Z. Liu, B. Han, T. Jiang, W. Wu, J. Chen, Z. Li, D. Liu, *J. Phys. Chem. B* **108**, 2200 (2004).
- [9] L. J. Zhang, M. X. Wan, *J. Phys. Chem. B* **107**, 6748 (2003).
- [10] D. H. Reneker, I. Chun, *Nanotechnology* **7**, 216 (1996).
- [11] H. X. He, C. Z. Li, N. J. Tao, *Appl. Phys. Lett.* **78**, 811 (2001).
- [12] R. Sen, B. Zhao, D. Perea, M. E. Itkis, H. Hu, J. Love, E. Bekyarova, R. C. Haddon, *Nano Lett.* **4**, 459 (2004).
- [13] J. Sun, William, W. Gerberich, Lorraine F. Francis, *J. Polym. Sci. Part B: Polym. Phys.* **41**, 1744 (2003).
- [14] W. Pan, H. Q. Zhang, Y. Chen, *J. Mater. Sci. Technol.* **25**, 247 (2009).
- [15] W. Pan, H. T. Zou, *Bull. Mater. Sci.* **31**, 807 (2008).
- [16] R. B. Mathur, O. P. Bahl, P. Sivaram, *Curr. Sci.* **62**, 662 (1992).
- [17] M. Panapoy, A. Dankeaw, B. Ksapabutr, *Int. J. Sci. Technol.* **13**, 11 (2008).
- [18] M. A. Phadke, S. S. Kulkarni, S. K. Karode, D. A. Musale, *J. Polym. Sci. Part B: Polym. Phys.* **43**, 2074 (2005).
- [19] X. Qu, T. Guan, G. Liu, Q. She, *J. Appl. Polym. Sci.* **97**, 348 (2005).
- [20] P. Cousin, P. Smith, *J. Polym. Sci. Part B: Polym. Phys.* **32**, 459 (2003).
- [21] C. Kim, Y. Jeong, B. T. Nhu-Ngoc, K. S. Yang, M. Kojima, Y. A. Kim, M. Endo, J. W. Lee, *Small* **3**, 91 (2007).
- [22] L. W. Ji, C. Saquing, S. A. Khan, X. G. Zhang, *Nanotechnology* **19**, 1 (2008).
- [23] L. L. Li, L. M. Mao, X. C. Duan, *Materials Research Bulletin* **41**, 541 (2006).

\*Corresponding author: panwei@zzti.edu.cn